Extended Abstracts of the 1992 International Conference on Solid State Devices and Materials, Tsukuba, 1992, pp. 170-172 **PA3-3**

A Closed-Loop Extraction of the Spatial Distribution of Interface Traps Based on Numerical Model of the Charge-Pumping Experiment

Predrag HABAŠ and Siegfried SELBERHERR

Institute for Microelectronics
Gusshausstrasse 27-29, 1040 Vienna, Austria/Europe

The extraction of the spatial distribution of interface traps from the experimental charge-pumping data is analysed in detail. The study is based on a numerical two-dimensional transient model of the charge-pumping experiment. The present trap extraction procedures are evaluated and improved; the derived expressions are confirmed by the rigorous numerical simulation on the models for virgin and stressed devices. The application of the model for the charge-pumping experiment to extract the spatial trap distribution in n-channel LDD devices after stress is presented.

1. Introduction and numerical model

Charge-pumping techniques have been extensively used to extract the spatial distribution of interface traps N_{it}[1-7] and fixed oxide charge[7-9] along the oxide/semiconductor interface in MOS devices before and after stress. The used extraction procedures are based on analytical expressions which rely on several approximations. According to our knowledge, no confirmation has been given for these methods in the literature. The accuracy of the obtained distributions $N_{it}(x)$ near/within the junctions is still unknown, because there is no method to measure $N_{it}(x)$ directly. In this paper a rigorous two-dimensional transient simulation of the charge-pumping (CP) experiment is used to evaluate the validity of the extraction procedures. The concept is presented in Fig.1. For an assumed distribution of interface traps and fixed oxide charge, we calculate numerically the charge-pumping current (e.g. I_{cp} versus source/drain junction reverse bias U_r) applying transient pulses at the device terminals. The calculated I_{cp} is further used instead of the experimental I_{cp} data, Fig.1. Comparing the extracted trap distribution with the assumed, we evaluated and improved the present techniques for the $N_{it}(x)$ extraction. The rigorous simulation of the CP experiment is implemented in MINIMOS[11]. It is based on: (1) The numerical solution of the time-dependent basic semiconductor equations. (2) Accurate terminal current calculation. (3) Trap dynamics is described by the Shockley-Read-Hall-like equations. The generation-recombination rates for electrons and holes are coupled with the transient continuity equations, while the dynamic trapped charge is coupled with the Poisson equation. The system is solved self-consistently. Arbitrary interface and volume trap distributions can be discretized in energy and position space. After a simulation lasting a few signal periods, the time averages of the terminal currents and the interface effective generation rates are calculated, taking care for the periodic steady-state condition. To the best of our knowledge, this approach accounts for the first time for the effects in the CP experiment related to a finite carrier response[11] (parasitic geometric current components in conventional MOSFET's and SOI devices), and for the 2D effects due to lateral nonuniform distribution of traps, variable charge-pumping threshold and flat-band voltages U_{th}^{cp} and V_{fb}^{cp} and, therefore, variable emission times $t_{em,n,p}$ within the junctions[10] (Fig.2).

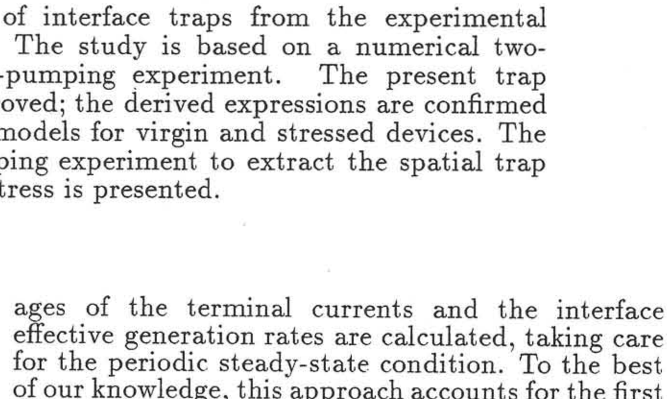

Fig.1 A closed-loop procedure to evaluate and improve the engineering methods for the extraction of trap distribution.

2. Trap distribution extraction

The mostly used CP technique will be analyzed: constant gate-bulk pulse train is applied, while the drain/source-bulk bias U_r is varied – method II[1,3]. With the reverse bias U_r the current I_{cp} changes due to two effects (n-channel devices):

1) The edges of the available area for the hole capture during the low gate-pulse level U_{GBl} at the

source x_s and the drain side x_d move with the reverse bias. These edges are defined by the critical hole concentration $p_s^{crit.}$[3,4] which is sufficient to refill all traps with holes during the gate base level. The relationships $x_{s,d}(U_r)$ can be obtained numerically by the standard method[1,3,4,6].

2) The CP threshold U_{th}^{cp} and the CP flat-band voltage V_{fb}^{cp} (in the junctions) are dependent on the reverse bias, Fig.2. Consequently, the emission times for electrons and holes $t_{em,n,p}$, and therefore the electron and hole emission levels $E_{em,n,p}$ change with U_r. This effect has been neglected previously in the literature. However, due to $U_{th}^{cp}(U_r)$, the contribution of the whole channel to the I_{cp} current changes with U_r. Note that the emission times are an explicit function of both the coordinate and the reverse bias, $t_{em} = t_{em}(U_r, x)$.

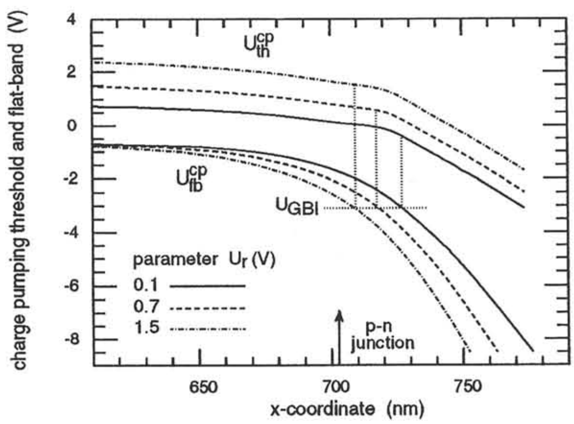

Fig.2 Charge-pumping flat-band and threshold voltage in the channel and within the drain junction.

For a symmetric case (virgin devices), $x_s = L_G - x_d$, the trap density D_{it} at $x_d(U_r)$ is given with

$$\int_{E_{em,p}(x_d,U_r)}^{E_{em,n}(x_d,U_r)} D_{it}(E, x_d)dE = \frac{1}{2fqW}\left[\frac{-\partial I_{cp}}{\partial U_r} + fqW\int_{x_s}^{x_d} \frac{\partial E_{em,n}}{\partial U_r}\left[D_{it}(E_{em,n}, x) + D_{it}(E_{em,p}, x)\right] dx\right] \cdot \left(\frac{-\partial x_d}{\partial U_r}\right)^{-1}$$

Neglecting the second term in the brackets, which represents a correction due to $t_{em}(U_r)$, the expression reduces to one used in the literature[5,6]. The second term can be approximated with the corresponding value for the channel. The last is obtainable either by numerical simulation assuming traps in the middle of the channel solely, or experimentally from the difference between $I_{cp}(U_r)$ for two devices produced simultaneously by the same technology with different channel length, $\Delta I_{cp}(U_r)$ (assuming close trap density distributions in both devices); the second term can be estimated then with $\partial(\ln \Delta I_{cp})/\partial U_r \cdot I_{cp}(U_r)$. An example is given in Fig.3. Dashed curve is an assumed nonuniform trap distribution in virgin device, which is used to calculate $I_{cp}(U_r)$ numerically. Dotted-dashed curve is recalculated assuming the term $-\partial I_{cp}/\partial U_r$ only. Accounting for the variable t_{em} the recalculated curve becomes close to the assumed distribution (solid lines). Note that the error due to neglecting the second term increases with increasing the channel length.

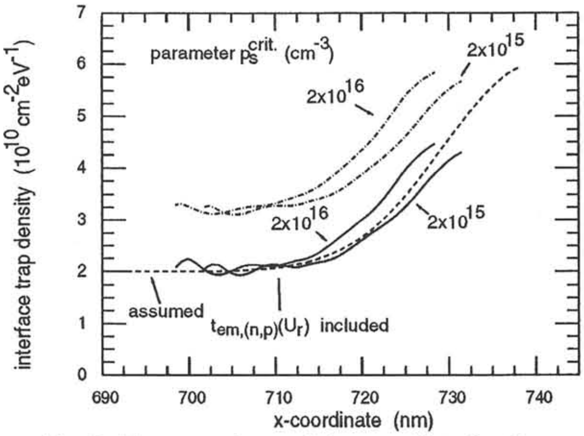

Fig.3 Extracted spatial trap distribution versus the assumed distribution in virgin device. $L_G = 0.8\mu m$.

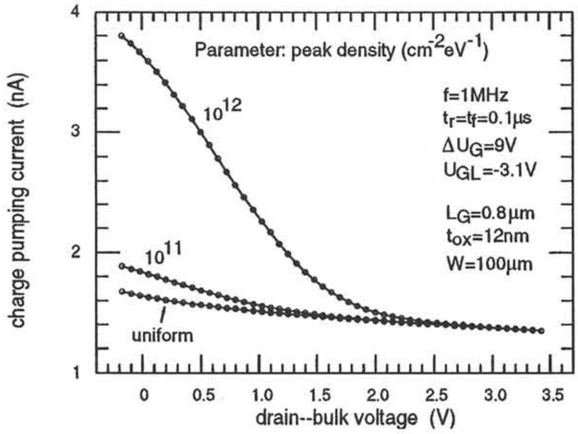

Fig.4 Calculated I_{cp} for the assumed model of virgin and stressed devices.

In the second example we consider stressed devices; a nonsymmetric case. Fig.4 shows the simulated $I_{cp}(U_r)$ curve for virgin device with a uniform trap distribution ($2\times10^{10} cm^{-2}eV^{-1}$), and for two stressed devices modeled by a superposed gaussian trap distribution within the drain junction (peak density 10^{11} and $10^{12} cm^{-2}eV^{-1}$; Figs.5,6) which location has been chosen relative to the electric-field peak at the stress bias according to the experimental observation[3]. Applying the extraction procedure on the difference between the current for the stressed device and the virgin device $\delta I_{cp}(U_r)$, instead on I_{cp}, the undesired contribution of the term due to the variable t_{em} in the channel can be made negligible. For the traps localized in a narrow interval, the change of I_{cp} with U_r is primarily due to the change of x_d, while the variation of t_{em} for traps which contribute to the CP current is a second order effect. The distributions, recalculated from the curves shown in Fig.4, are given in Figs.5 and 6. Contrary to the claim in the literature[3,4], the parameter $p_s^{crit.}$ ought to be chosen carefully; it determines the location of the extracted peak[3]. We found that the value of $p_s^{crit.}$

which corresponds to 3 hole-capture time constants during the gate pulse base-level U_{GBl} (in this case $2 \times 10^{16} cm^{-3}$), leads to a shift to the left from the assumed distribution. This shift is partially due to a finite width of the transition between the active and the non-active CP area (which is not a step-like function). The small discrepancy in the amplitude originates due to the longer emission times t_{em} associated with traps in the junction than with that in the channel (used in the recalculation), Fig.2. In conclusion, our study has confirmed the ability to extract accurately the spatial trap distribution by using the CP method discussed (assuming proper $p_s^{crit.}$).

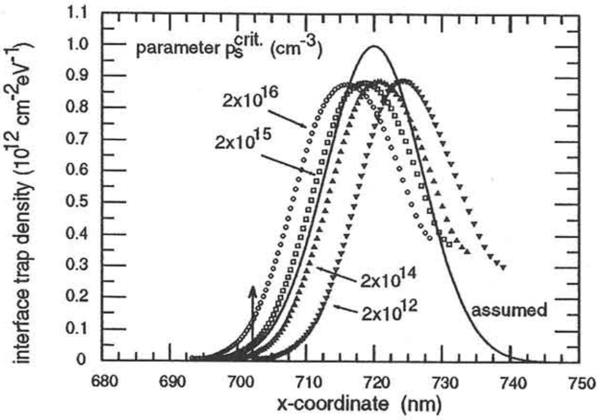

Fig.5 Extracted spatial trap distribution versus the assumed gaussian distribution for the additional stress-generated traps. $L_G = 0.8\mu m$. Drain junction is located at $0.702\mu m$.

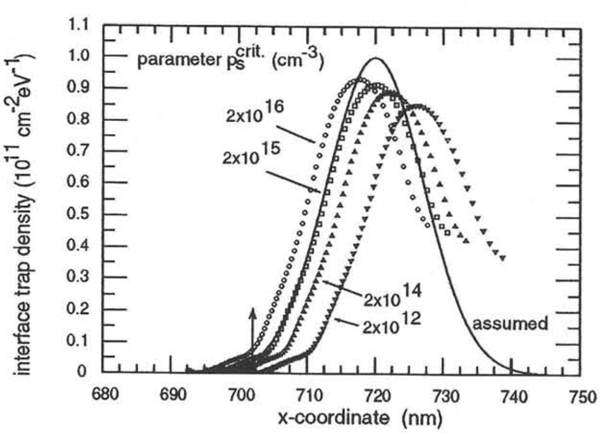

Fig.6 Extracted trap distribution for a low density of the generated traps.

The variation of the emission times influences I_{cp} in other CP methods used to scan the lateral trap profile, like the method I[1], two-pulse modification[3], the technique with fixed gate base-level and variable top-level[2] and with fixed gate top-level and variable base-level[7,8] (n-channel), as well. In the last two methods, this undesired effect can be eliminated by keeping the pulse slope $\Delta U_G/t_{r,f}$ constant[8]. However, this effect does not exist in the simple conventional technique[10] with constant ΔU_G, t_r, t_f and U_r, and variable gate base/top-level, with keeping the gate top-level in inversion.

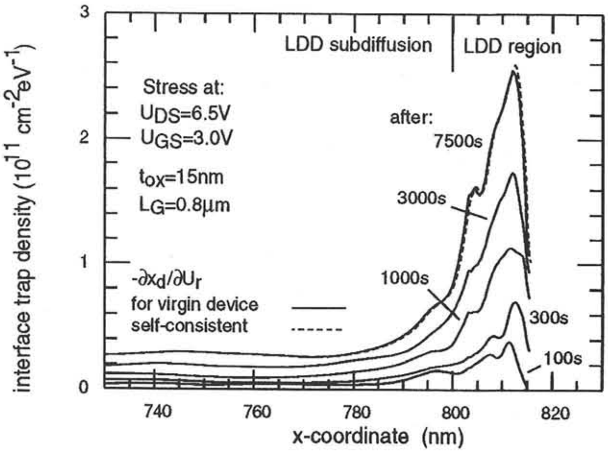

Fig.7 Trap distribution in n-channel LDD device stressed at $U_{DS} = 6.5V$, $U_{GS} = 3V$.

Using the last CP method we extract the spatial trap distribution in n-channel LDD device after the hot-carrier stress at maximum I_B, Fig7. Moreover, for the extracted trap distribution, I_{cp} can be calculated numerically using the rigorous transient model of the CP experiment, and then compared with the experimental I_{cp}. The obtained agreement confirms the accuracy of the trap distribution obtained, which is, however, dependent on the accuracy of the lateral impurity profile in the subdiffusion region. Note that a 2D transient approach is indispensible to calculate the complete $I_{cp}(U_{GBl})$ curve for LDD devices due to the gate-edge/LDD-region fringing effect.

Acknowledgements: We would like to thank G. Groeseneken and his group for discussions and for providing us with experimental data. Our work is supported by Siemens Corporation at Munich, FRG; Digital Equipment Corporation at Hudson, MA; and Sony Corporation at Atsugi, Japan.

References

1) T.Poorter and P.Zoestbergen; IEDM Tech.Dig. (1984) 100.
2) G.Dalla Libera and C.Bergonzoni; ICVC Proc. (1991) 183.
3) M.G.Ancona, N.S.Saks and D.McCarthy; IEEE Trans. Electron Dev. ED 35 (1988) 2221.
4) N.S.Saks and M.G.Ancona; IEEE Trans. Electron Dev. 37 (1990) 1057.
5) X.M.Li, M.J.Deen; IEDM Tech.Dig. (1990) 85.
6) J.-J.Shaw, K.Wu; IEDM Tech.Dig. (1989) 83.
7) R.Mahnkopf, G.Przyrembel and H.G.Wagemann; ESSDERC (1988) 775.
8) M.Tsuchiaki, H.S.Momose, T.Morimoto and H.Iwai; Symp. on VLSI Techn. (1991) 19.
9) W.Chen and T.-P.Ma; IEEE Electron Dev. Lett. 12 (1991) 393.
10) P.Heremans, J.Witters, G.Groeseneken, H.E.Maes; IEEE Trans. Electron Dev. 36 (1989) 1318.
11) P.Habaš, O.Heinreichsberger and S.Selberherr; ESSDERC (1992) will be presented.
12) D.Vuillaume, J.C.Marchetaux and A.Boudou; IEEE Electron Dev. Lett. 12 (1991) 60.